Promotion Effects of Nickel Catalysts of Dry Reforming with Methane

YAN, Zi-Feng*(阎子峰) DING, Rong-Gang(丁荣刚) LIU, Xin-Mei(刘欣梅)
SONG, Lin-Hua(宋林花)
State Key Laboratory for Heavy Oil Processing, University of Petroleum, Dongying, Shandong 257061, China

The promotion effects of nickel catalyst of dry reforming with methane were extensively investigated by means of XRD, SEM, EDX, N_2-adsorption and H_2-adsorption. XRD characterization indicated that good dispersion of nickel oxide and MgO promoter is achieved over γ-Al_2O_3 support. Addition of MgO promoter effectively retards the formation of $NiAl_2O_4$ phase. SEM and EDX analysis exhibited that the addition of rare-earth metal oxide CeO_2 effectively promotes the Ni metal dispersion on the surface of the catalysts despite of undesirable self-dispersion of CeO_2 promoter. Furthermore, the nickel component is gradually dispersed on the surface of the support following the exposure to reaction gas mixture for a period of time. The addition of MgO inhibited the self-dispersion and promotion effect of CeO_2 on Ni dispersion on the catalysts. H_2 chemisorption revealed that the addition of the alkaline oxide MgO promoter significantly prohibits the metal dispersion on the catalyst. Inappropriate promoter addition can result in sharp decrease of the metal dispersion. N_2-adsorption indicated that oxide promoter was mostly concentrated on the outer layer of the alumina support while the nickel metal was generally dispersed in the support pores. Addition of promoters contributed to more reduction in mesopore volume.

Keywords Promotion effect, dry reforming with methane, catalyst, carbon deposition

Introduction

The dry reforming is a little higher endothermic reaction than steam reforming:

$$CO_2 + CH_4 \rightarrow 2\ CO + 2\ H_2 \quad \Delta H^0_{298} = 247\ kJ/mol$$

The dry reforming with methane was firstly proposed by Fischer and Tropsch in 1928.[1,2] Renewed interest in this conversion has been ascribed to its potential use for industry and energy storage as well as the associated environmental benefits. The significance of this reforming reaction lies in that it utilizes carbon dioxide and methane, which are two potential greenhouse gases, while it produces syn-gas, a valuable chemical feed gas. Furthermore, The CO-rich synthesis gas supplied by this reaction is desired for the production of oxygenated derivatives. Carbon deposition over catalysts is the fatal problem for carbon dioxide reforming with methane. Although some noble metals show high activity and selectivity for carbon-free operation, high cost and limited availability of noble metals prevent the commercial use of this reaction. It is, therefore, more practical to develop an improved nickel-based catalyst which exhibits stable operation for a long period of time.

Addition of alkali promoter to catalyst was effective in preventing coke formation from methane during steam reforming. Similarly, for the reaction of CO_2 reforming with methane, adding basic promoter such as alkali or alkali-earth oxides may also change the nature of the support, because CO_2 is adsorbed strongly on the surface of basic catalysts and covers a large part of the surface at lower CO_2 partial pressure. Yamazaki[3] developed a catalyst of Ni/MgO-CaO. It showed that high basicity and lower coke formation ability attributed to the addition of CaO. Activity of the Co-MgO/C system was compared

* E-mail: zfyan@hdpu.edu.cn
Received October 19, 2000; revised March 12, 2001; accepted April 2, 2001.
Project supported by the Shandong Foundation of Outstanding Young Scientists and the Innovation Foundation of Young Scientists, China National Petroleum Corporation (No. 970405).

with that of Co/C catalyst and the results suggested that the role of MgO is to avoid occurrence of the Boudouard reaction. Ni-CaO/Al_2O_3 catalyst was also found to have higher reaction rate and stability than Ni/Al_2O_3. This is related to a relatively enhanced reactivity of the C_β and C_γ deposited on the catalyst.[4,5]

Experimental

Catalyst preparation

The supported nickel catalysts were prepared by a conventionally incipient wetness impregnation method, with aqueous solutions of nitrates as promoter and metal precursors.

Catalyst evaluation

The catalyst was reduced in a stream of H_2 for at least 2 h under the carbon dioxide reforming reaction conditions in the micro-reactor before the reaction. Activity measurements were carried out in the continuous flow quartz-fixed-bed reactor (*i. d.*, 6 mm) under atmospheric pressure, at various reaction temperatures and feed ratios of the reactant mixture.

The composition of reactants/products mixture was analyzed using thermal conductivity detector of an on-line SP-3420 gas chromatography. A Porapak QS100/120 column was used to separate the effluent gas of H_2, CO, CH_4, and CO_2.

Catalyst Characterization

X-ray powder diffraction (XRD)

A BDX-3200 X-ray powder diffractometer, manufactured by Peking University Instrument Factory, was used to identify the main phases of nickel-based catalysts. Anode Cu K_α(40 kV, 20 mA) was employed as the X-ray radiation source, covering 2θ between 20° and 80°.

SEM *and* EDX

The microscopic appearance observation was conducted using scanning electron microscope (JEM 5410LV, JEOL Technologies) with the accelerating voltage of 25 kV. The surface elemental composition of the catalysts was determined by energy distribution spectrum using X-ray microanalysis (ISIS, Oxford Instrument). The SiLi detector was employed and the elements with atomic number above 4 (B element) in the element periodic table can be detected.

Surface area and porosimetry

The surface properties such as surface area, average pore diameter, and pore volume were determined using a gas sorption analyzer using N_2 adsorption at 77.5 K. The accelerated surface area and porosimetry analyzer (ASAP 2010) were manufactured by Micromeritics Corporation in U.S.A.

From the adsorption isotherm, surface area was determined using the BET equation. The total pore volume was derived from the amount of adsorption at a relatively pressure close to unity. The mesopore volume/area and pore distribution curve were obtained from the adsorption branch of the N_2 isotherm by BJH method.

Detection of metal dispersion

The dispersion of nickel on the support was roughly estimated by static equilibrium chemisorption of H_2 at rather isothermal conditions of 308 K. A constant volume high-vacuum apparatus (Micromeritics, ASAP 2010C) was used for this purpose. Before analysis, samples were degassed under vacuum for 1 h at 373 K and 3 h at 673 K. The prepared catalyst samples were weighed and quickly transferred to the analysis port.

Results and discussion

Effects of promoter on catalysts

As usual, the activity of the metal catalyst is affected by the combination of metal, support and promoters. Fig. 1 showed the influence of promoter on the catalytic performance. The methane conversions obtained over CeO_2 and K_2O-promoted catalysts were found to be slightly lower than that over w = 8.5% Ni/Al_2O_3 catalyst, a result that was expected in view of previous observations that the presence of basic promoters leads to a reduction of catalyst activity. The decreasing rates of ac-

tivity over promoted catalysts were lower than that over the unpromoted catalyst. The methane conversions over K_2O and CeO_2 modified catalysts decreased by 10.5% and 16.2%, respectively. Addition of promoters may block parts of metallic Ni sites and thus result in a reduction of methane conversion.

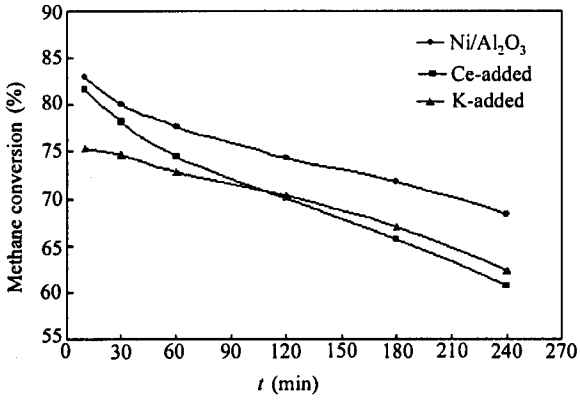

Fig. 1 Variation of methane conversion over promoted nickel catalyst. $w(Ni) = 8.5\%$, $P = 1 \times 10^5$ Pa, $T = 973$ K, $n(CH_4/CO_2) = 1.05$, WHSV = 12.5 h^{-1}.

It was also observed that catalyst deactivation was reduced indeed by adding CeO_2 and K_2O. The K_2O promoter exhibited more effective inhibition to carbon deposition on the catalyst surface than CeO_2.

XRD *characterization*

The XRD patterns of the support, the promoted and unpromoted nickel based catalysts were shown in Fig. 2. From the comparison of the XRD spectra of support and catalysts, it was clearly observed that NiO diffraction peak appeared in the spectra of neither unpromoted nor promoted nickel based catalysts. It was a good indication that high dispersion of nickel oxide was achieved over γ-Al_2O_3 support.

As can be derived from the XRD spectra shown in Fig. 2, there exists no detectable solid reaction between NiO and Al_2O_3 over promoted catalyst. However, certain amounts of nickel were found in the form of $NiAl_2O_4$, a compound resulting from the solid reaction between NiO and the acidic Al_2O_3 support in the Ni/Al_2O_3 catalyst. The $NiAl_2O_4$ crystalline phase, which has a stable spinel structure, is rather difficult to be reduced, as witnessed by the fact that it essentially survives H_2 reduction at 1023 K.[6] However, addition of MgO ($w = 3\%$) to γ-Al_2O_3 significantly affects the basicity/acidity of the support, leading to a profound change in the bulk phase composition. It was observed that the diffraction peak of $NiAl_2O_4$ disappeared over alkaline metal oxide promoted catalyst. This is probably attributed the fact the basic MgO is preferably reacting with the acidic Al_2O_3 to form stable magnesium aluminate, thereby suppressing the reaction between NiO and Al_2O_3.

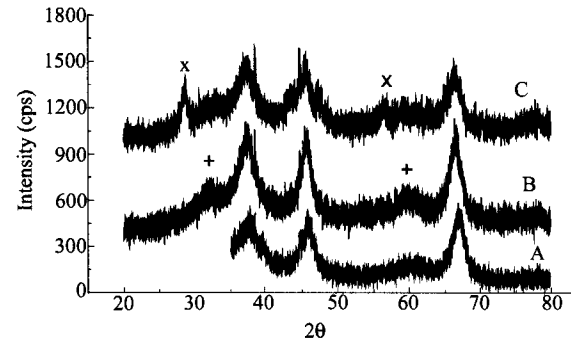

Fig. 2 XRD patterns of Al_2O_3 support, unpromoted and promoted catalysts calcined at 873 K. A: γ-Al_2O_3; B: 8.5% Ni/γ-Al_2O_3; C: Ni(8.5%)-MgO(2%)-CeO_2(3%)/γ-Al_2O_3; +: $NiAl_2O_4$; ×: CeO_2.

The emergence of CeO_2 diffraction peak in Ni-Mg-Ce/Al_2O_3 catalyst indicated that the dispersion of CeO_2 was undesirable. This may be related to the catalyst preparation processes and conditions. More series tests of the influence of CeO_2 addition on the dispersion of metal are absent now. The well dispersion of appropriate CeO_2 addition with or without other promoters is also an interesting topic worth further studying. The Ni-Mg-Ce/Al_2O_3 catalyst exhibited perfect performance in the catalyst evaluation experiments despite of undesirable dispersion of CeO_2 promoter. The EDX analysis explains the emergence of the CeO_2 diffraction peak perfectly in following section. In the sharp contrast to CeO_2, the dispersion of MgO promoter was satisfactory and no diffraction peak appeared in the XRD patterns of the promoted catalyst.

SEM *and* EDX *analysis*

The surface elemental compositions of the fresh and used catalysts were characterized by EDX analysis and the results were shown in Tables 1 and 2. Table 1

showed the relative content of selected elements and Table 2 showed the full element composition of surfaces of the catalysts.

Table 1 Surface composition of fresh and used nickel catalysts[a]

Catalyst	State	Al (%)[b]	Ni (%)[b]	Mg (%)[b]	Ce (%)[b]
7% Ni/Al_2O_3	fresh	94.71	5.29	------	------
	used	97.63	2.37	------	------
Ni(8.5%)-MgO(2%)-CeO_2(3%)/Al_2O_3	fresh	84.31	9.18	n.d.[c]	6.51
	used	84.74	10.61	n.d.[c]	4.65
Ni(10%)-MgO(2%)/Al_2O_3	fresh	94.26	5.74	n.d.[c]	------
	used	95.80	4.21	------	------
Ni(11.5%)-CeO_2(3%)/Al_2O_3	fresh	93.04	4.18	------	2.78
	used	89.97	4.85	------	5.19

[a] $P = 1 \times 10^5$ Pa, $T = 973$ K, $n(CH_4/CO_2) = 1.05$, WHSV = 12.5 h^{-1}, used for 4 h; [b] atomic percentage; [c] not detected.

Table 2 Surface composition of nickel catalysts before and after reaction[a]

Catalyst	State	Al (%)[b]	Ni (%)[b]	Mg (%)[b]	Ce (%)[b]	Si (%)[b]	Na (%)[b]	C (%)[b]	O (%)[b]
Ni(7%)-MgO(3%)-CeO_2(3%)/SiO_2	fresh	----	6.95	1.65	0.35	18.4	----	----	72.7
	used	----	3.38	0.22	0.11	4.36	----	80.3	11.6
Ni(8.5%)-MgO(3%)-CeO_2(3%)/Al_2O_3	fresh	25.4	2.8	1.21	0.48	----	2.83	----	67.3
	red.	27.7	2.96	1.29	0.83	----	2.26	----	65.0
	used	15.6	2.06	0.67	0.32	----	1.72	21.5	58.1
Ni(8.5%)-MgO(2%)-CeO_2(3%)/Al_2O_3	fresh	25.5	3.38	0.43	0.38	----	0.46	----	68.5

[a] $P = 1 \times 10^5$ Pa, $T = 973$ K, $n(CH_4/CO_2) = 1.05$, WHSV = 12.5 h^{-1}, used for 4 h; [b] atomic percentage.

The high surface concentration of some element indicates that uniform dispersion of the element is achieved. The enrichment trend of the element may be effectively retarded and various states of the element essentially exist in relatively small particles. From Table 1 it was observed that the surface concentration of the Ni over unpromoted catalyst significantly decreased by almost one time, from 5.29% to 2.37%, after carbon dioxide reforming reaction. The surface concentration of Ni element also declined to some extent, from 5.74% to 4.21% over the MgO promoted catalyst after reaction. However, it was interesting that the surface concentrations of Ni element increased over CeO_2 promoted catalysts after reaction.

For the Ce-promoted catalysts, the nickel loadings on the support were higher than that of Ce-deficient catalysts. High nickel loading does not favor the dispersion of Ni on the surface of the support. However, the surface concentration of Ni reached 4.18% on the fresh Ni (11.5%)-Ce(3%)Al_2O_3 catalyst, approached that on the fresh 7.5% Ni/Al_2O_3 catalyst. The uniform dispersion of nickel component over the 8.5% Ni loaded catalyst might be ascribed to appropriate nickel loading. Lu studied the optimum nickel loading on various supports.[7] The results showed that two-dimensional surface compound was formed by the interaction between NiO and Al_2O_3 with nickel loading set at 9.0% under the specific conditions. The large Ni particles provided less active metal surface area and caused rapid deactivation by carbon deposition on the Ni particles.

The high surface concentration of Ni on the Ni (8.5%)-MgO(2%)-CeO_2(3%)/Al_2O_3 may be derived from two causes. The appropriate nickel loading was the key to obtaining uniform dispersion on the surface of the Al_2O_3 support. As mentioned above, two-dimensional surface compound may be formed by the interaction between NiO and Al_2O_3 on the catalyst and Ni particles were highly dispersed under the specific conditions. Additionally, the comparison of the surface compositions of the catalysts gave good indication that the addition of

rare-earth metal oxide CeO_2 effectively promoted the Ni metal dispersion on the surface of the catalysts. Furthermore, the nickel component was gradually dispersed on the surface of the support following the exposure to reaction gas mixture for a period of time.

It was also noteworthy that the change of the self-dispersion of CeO_2 on the support. The surface concentration of Ce decreased from 6.51% to 4.65% on the MgO-containing catalyst and increased from 2.78% to 5.19% on the MgO-deficient catalyst after reaction. The surface concentration of Ce decreased from 6.51% to 4.28% when the MgO addition increased from 2% to 3% for the fresh catalysts. Apparently, the addition of MgO inhibited the self-dispersion of CeO_2 on the catalysts. Therefore, the appearance of CeO_2 diffraction peak on the XRD patterns of Ni(8.5%)-MgO(2%)-CeO_2(3%)/Al_2O_3 catalyst was indicative of the undesirable self-dispersion of CeO_2 promoter. The EDX analysis result by scanning electron microscope was in good harmony with the XRD experiment result.

The surface concentration of Mg was not detected on the catalysts below 2% MgO added. The comparison of the Ni-Mg-Ce/Al_2O_3 catalyst with different MgO content exhibited that increased MgO addition inhibited the promotion effect of CeO_2 on Ni dispersion. Therefore, the optimum combination of the addition amount of the promoters is very important for perfect metal dispersion and desirable catalyst performance in the carbon dioxide reforming with methane.

The nickel dispersion of the catalyst on alumina support was less than that on silica support (Fig. 3). This may be due to the strong interaction between nickel and alumina and undeveloped support pore structure than is silica. However, high catalytic activity and resistivity to carbon deposition were obtained on the nickel catalyst supported on alumina. This indicated that metal dispersion was not the decisive factor that influenced the catalyst performance.

The metal dispersion of the Ni-Mg-Ce/Al_2O_3 catalyst was slightly improved after H_2 reduction at high temperature, with Ni surface concentration increased from 2.80% to 2.96%. The Ni surface concentration declined to 2.06% after reaction. This was mainly the partial coverage of carbonaceous species on the surface active sites of the used catalyst. The carbon surface concentration, 26.7%, was much less than that on Ni-Mg-Ce/SiO_2 catalyst.

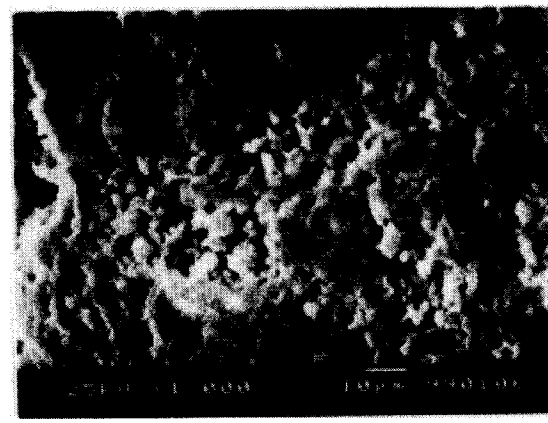

Fig. 3 SEM photo of reduced Ni(8.5%)-MgO(3%)-CeO_2(3%)/Al_2O_3 catalyst.

Severe carbon deposition occurred on the Ni-Mg-Ce/SiO_2 catalyst and the surface concentration of carbon reached 80.3% although nickel was highly dispersed (as showed in Fig. 4). The results indicated that the surface carbon was the dominant element on used Ni-Mg-Ce/SiO_2 catalyst. The carbon deposition resulted in the significant decrease of the surface concentrations of Ni, Mg, and Ce. The variation of surface elemental concentration gave good evidence that carbon deposit not only on the surfaces of metal active sites but also on the support.

Fig. 4 SEM photo of used Ni(8.5%)-MgO(3%)-CeO_2(3%)/Al_2O_3 catalyst.

Nickel crystalline size of the used catalyst was increased indicating that sintering of catalyst occurred in the tested catalyst. Fig. 4 showed that the degree of sintering was not so appreciable for Ni-Mg-Ce/Al_2O_3.

Metal dispersion

Table 3 showed that the metal dispersions of Ni and metallic surface areas on all catalysts were not very high. The apparent low nickel dispersion on the high surface area of γ-Al_2O_3 carrier was probably due to the formation of $NiAl_2O_4$, which is not capable of chemisorbing hydrogen at room temperature. Incomplete reduction of Ni crystalline particles, as well as blocking and coverage of nickel crystallites by species originating from MgO and CeO_2 promoters, may also contribute to lowering the amount of hydrogen adsorbed.

Table 3 Metal dispersions and metallic surface areas of the catalysts

Catalyst	M_{disp} [a] (%)	M_{sa} [b] (m^2/g sample)	M_{sa} [c] (%/m^2)
Ni(8.5%)-MgO(2%)-CeO_2(3%)/Al_2O_3	0.313	0.177	2.081
Ni(8.5%)-MgO(3%)-CeO_2(3%)/Al_2O_3	0.113	0.064	0.752
Ni(7%)-MgO(1%)-CeO_2(1%)/Al_2O_3	0.204	0.095	1.354
Ni(10%)-MgO(2%)/Al_2O_3	0.170	0.114	1.134

[a] metal dispersion; [b] specific metallic surface area; [c] metal dispersion on per specific metal surface area.

The results showed that the Ni(8.5%)-MgO(2%)-CeO_2(3%)/Al_2O_3 catalyst achieved best metal dispersion among the tested catalysts. The nickel dispersion declined form 0.313% to 0.113% with increased MgO addition from w = 2% to 3%. This may be attributed partly to the catalyst preparation uncertainty. However, no doubt that the cause for the decrease of metal dispersion lies in the inappropriate promoter addition. EDX results also indicated that the surface nickel concentration of 2% MgO added catalyst was higher than that of 3% MgO added catalyst. It was in good accordance with the metal dispersion analysis by H_2 chemisorption.

Surface and porosity features

The adsorption isotherms of the untreated alumina, unpromoted and promoted catalysts were analyzed. All adsorption isotherms were similar to a type I isotherm. Impregnation resulted in an approached decrease in the amount adsorbed, with only slight modification of the knee corresponding to microporosity. Fig. 5 showed that mesopore distribution of the untreated, unpromoted and promoted catalysts. The variation of surface areas and total pore volumes of fresh and used catalysts with promoter addition were shown in Table 4.

Table 4 Characterization of catalyst pore structure

Catalyst	State	S_{BET} (m^2/g)	D [a] (A)	V_{total} (cm^3/g)	V_{micro} (cm^3/g)	V_{meso} (cm^3/g)
γ-Al_2O_3		192.4	62.5	0.300	0.054	0.246
7% Ni/Al_2O_3	fresh	171.7	56.3	0.242	0.047	0.195
	used	143.0	53.6	0.192	0.038	0.154
Ni(7%)-Mg(1%)-Ce(1%)/Al_2O_3	fresh	179.6	55.3	0.240	0.045	0.195
Ni(8.5%)-Mg(2%)-Ce(3%)/Al_2O_3	fresh	149.5	59.4	0.227	0.038	0.189
	used	125.8	72.0	0.226	0.033	0.193
Ni(8.5%)-Mg(3%)-Ce(2%)/Al_2O_3	fresh	148.3	57.0	0.212	0.039	0.173
Ni(8.5%)-Mg(3%)-Ce(3%)/Al_2O_3	fresh	129.7	64.0	0.200	0.034	0.166
Ni(10%)-Mg(3%)-Ce(1%)/Al_2O_3	fresh	143.7	63.3	0.227	0.036	0.191
	used	123.0	69.0	0.212	0.032	0.181
Ni(11.5%)-Mg(1%)-Ce(2%)/Al_2O_3	fresh	144.6	61.7	0.223	0.037	0.186
	used	126.6	73.5	0.232	0.033	0.199
Ni(11.5%)-Ce(3%)/Al_2O_3	fresh	142.5	71.5	0.255	0.036	0.219

[a] average pore diameter.

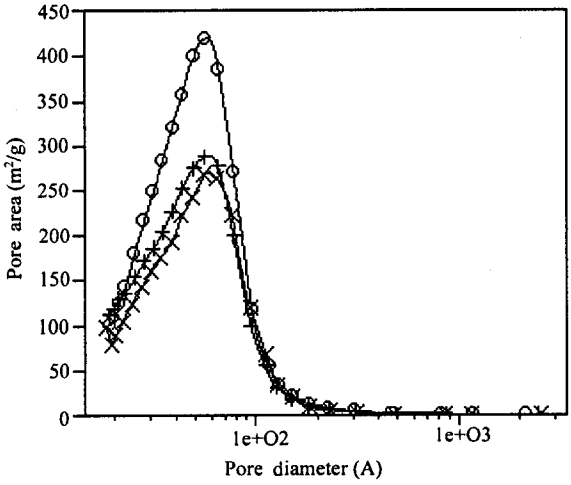

Fig. 5 Mesopore distribution of the untreated support and promoted Ni supported catalysts. ○: untreated γ-Al_2O_3; +: fresh Ni(11.5%)-MgO(1%)-CeO_2(2%)/Al_2O_3; ×: fresh Ni(11.5%)-CeO_2(3%)/Al_2O_3.

The unpromoted and promoted $w = 7\%$ Ni catalysts showed very slight difference in micro- and mesopore volume, but the variations were negligible and well within experimental errors. There was slight increase in surface area by promoter's addition. Fig. 5 indicated that the generation of the pores in the range of 10—30 A resulted in the increase of surface area. The part blocking of the bigger mesopores by oxide promoters may be responsible for the generation of smaller mesopores.

The pore structure variations of three kinds of $w = 8.5\%$ Ni catalysts in Table 4 and Fig. 5 showed that more promoter addition resulted in more decrease in mesopore volume and the MgO addition exhibited stronger effect on this decrease. The data for $w = 11.5\%$ Ni catalysts also indicated that MgO addition significantly influenced pore structure. Too MgO addition may retard the reduction of NiO and cover the NiO layer on the support surface. Therefore, inappropriate MgO addition may decrease the nickel dispersion and surface nickel concentration, which had been described in the H_2 chemisorption and EDX studies, thus affected the catalyst performance.

The promotion effect of nickel caltalyst with MgO and CeO_2 might be illustrated as Fig. 6.

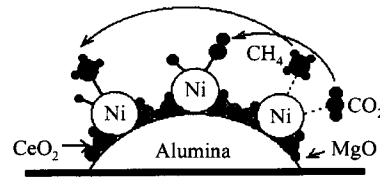

Fig. 6 Promotion sketch of nickel catalyst with MgO and CeO_2.

Conclusions

(1) XRD characterization indicated that the good dispersion of nickel oxide and MgO promoter is achieved over γ-Al_2O_3 support. Addition of MgO promoter effectively retards the formation of $NiAl_2O_4$ phase.

(2) The addition of rare-earth metal oxide CeO_2 effectively promotes the Ni metal dispersion on the surface of the catalysts despite of undesirable self-dispersion of CeO_2 promoter. The addition of MgO inhibited the self-dispersion and promotion effect of CeO_2 on Ni dispersion on the catalysts.

(3) The addition of the alkaline oxide MgO promoter significantly prohibits the metal dispersion on the catalyst. Inappropriate promoter addition can result in sharp decrease of the metal dispersion.

(4) The impregnated metal species maybe mainly locate on the inner surface of the micropore of the alumina support and that the reforming active sites also locate in these micropore metal sites.

References

1 Fischer, V. F.; Tropsch, H. *Brennst. Chem.* **1928**, *3*, 39.
2 Ross, J. R. H.; Kenlen, A. N. J.; Hegarty, M. E. S.; Seshan, K. *Catal. Today* **1996**, *30*, 193.
3 Yamazaki, O.; Nozaki, T.; Omata, K.; Fujimoto, K. *Chem. Lett.* **1992**, 1953.
4 Zhang, Z.; Verykios, X. E. *Catal. Today* **1994**, *21*, 589.
5 Sun, Q.; Li, W. Y.; Xie, K. C. *Ranliao Huaxue Xuebao* **1996**, *24*, 219 (in Chinese).
6 Zhang, Z. L.; Verykios X. E.; MacDonald, S. M.; Affrossman, S. *J. Phys. Chem.* **1996**, *100*, 744.
7 Lu, Y.; Yu, C. C. *Chin. J. Catal.* **1996**, *17*, 212(in Chinese).

(E200010225 LI, L.T.; LING, J.)